X-ray Diffraction and Mercury Porosimeter Examination of Metal Impregnated γ-Alumina Samples

[1]A. K. KHATTAK*, [1]K. MAHMOOD, [2]M. AFZAL, [2]M. SALEEM AND [3]R. QADEER
[1]*Department of Chemistry, Gomal University, Dera Ismail Khan (Pakistan)*
[2]*Department of Chemistry, Quaid-i-Azam University, Islamabad (Pakistan)*
[3]*Pakistan Atomic Energy Commission, P. Box, 1331, Islamabad (Pakistan)*

(Received 8th April, 2002, revised 15th March, 2003)

Summary: A series of metal impregnated alumina has been prepared by simple impregnation method of the host oxide (γ-alumina). In the present paper, two techniques, X-Ray Diffraction and Mercury Porosimeter have been applied for examining the effect of different concentrations of transition metals (Cr, Mn, Fe and Co) loaded on γ-alumina.

Introduction

Porous solid materials play an important role in technology having many ramifications throughout the economy. They are encountered widely in the chemical process industry, in pollution control, in life support systems, and in chemical research. Among the specific applications of porous solids are filters, adsorbents, chromatographic column packing, and catalyst support [1]. Alumina is a porous solid material. It has a large surface area and adsorption capacity. Alumina is of high practical importance because it serves as adsorbent in separation processes, as catalysts, and most importantly as support materials for catalyst such as transition metals and metal oxides [2, 3]. Alumina, due to its porous nature and catalytic behavior, is frequently employed to remove toxic and health hazardous particles and ions from gases and solutions at appropriate temperatures. As a support or as a co-catalyst, it is used in many catalytic processes of industrial importance [4,5].

The efficiency of alumina [6,7] as an adsorbent is based on the sizes and shapes of the pores which play an important role in physical adsorption, chemisorption and catalysis. In order to improve the efficiency of alumina as an adsorbent, it is loaded with certain metals. In the present work, alumina is loaded/doped with Cr, Mn, Fe and Co and as a result new surface is created. The thermodynamic and kinetic properties of the new surface are changed and are quite different from the parent alumina. The metals used for doping are also generally found to be effective adsorbents, on which not only adsorption, but also chemical reactions and catalytic decomposition of different gases can take place [8].

Adsorption of *n*-aliphatic alcohols on metal impregnated alumina samples and the determination of surface area applying the two most common methods i.e. the Langmuir method and the BET method has been studied extensively elsewhere by the authors [9]. Pore structure, total pore area, average pre diameter, BET surface area and total micropore volume for metal doped alumina samples containing different concentrations of metals with special reference to manganese has been investigated previously by mercury penetration using mercury porosimeter and low temperature nitrogen adsorption using Quantasorb Sorption System [10]. Comparative study of the adsorption of *n*-aliphatic alcohols on metal impregnated alumina samples has been made [11]. In addition, the nature of the parent and of the impregnated alumina samples has been investigated by Thermogravimetry (TG), Differential Thermogravimetric Analysis (DTA) and Derivative Thermogravimetry (DTG).

However, in the present study, two techniques, x-ray diffraction and mercury porosimeter have been applied for examining the surface of parent and metal impregnated γ-alumina samples. X-ray diffraction is a powerful technique used to determine crystal structure. It provides more structural informations as compared to other scientific techniques [12]. Using x-ray technique, the average particle size can be estimated by two methods. These are (1) low angle scattering of the x-rays and (2) x-ray line broadening analysis (XLBA). In the present work, this technique (XLBA) has been employed to measure crystallite size of the parent and metal impregnated alumina samples. In addition, purpose of the x-ray diffraction experiment has been to obtain the x-ray diffraction

*To whom all correspondence should be addressed.

pattern of the powdered crystalline material belonging to the cubic system (γ-alumina). From the experimental data, including a separate density measurement, the interlayers spacing, unit cell constant (a), unit cell volume (a^3) and crystallite size (d) have been determined.

Mercury Porosimeter is an analytical technique which is used to determine usually the size, shape and features of porous materials. Mercury penetration technique is more rapid, covenient and accurate way to determine the pore size distribution in the large pore range [1, 13]. This technique was suggested first by authors [14] and was used by Ritter and Drake [15]. Ritter and Drake proved the usefulness of measuring the penetration of mercury under pressure in order to elucidate the pore size distribution of various substances. This technique was first applied to the determination of large pores in charcoal by Emmett and his Co-workers [16]. In this method, the pressure required to force measured volumes of mercury into pores is determined. From this information, the volume of each size of pore in the sample can be determined [17]. In the present paper, work has been done on the pore size distribution of metal impregnated alumina samples with special reference to chromium metal. The purpose of the present paper is to amplify the information regarding the pore shape and total pore area for parent and metal doped alumina given in our previous publication [10].

Reported measurements [18-21] of contact angles between mercury and a large variety of materials range from 112 to 142° being the most frequently encountered value. In the absence of specific information about the contact angle, a value of 130° is usually adopted; however, use of incorrect value can give rise to large differences in apparent pore diameter. In the recent years, some workers [1] preferred the value θ = 130°. In the current work, contact angle 130° has been used for mercury porosimetric measurements.

Results and Discussion

The structure of gamma alumina (γ-Al_2O_3) generally accepted to be a cubic structure of the spinel type [22-24]. The side of the unit cube is given as 7.84 A°, to explain the observed density, a defect type structure must be assumed.

Fig. (1) reports the XRD spectrum for parent alumina and for comparison, the spectra of all metal

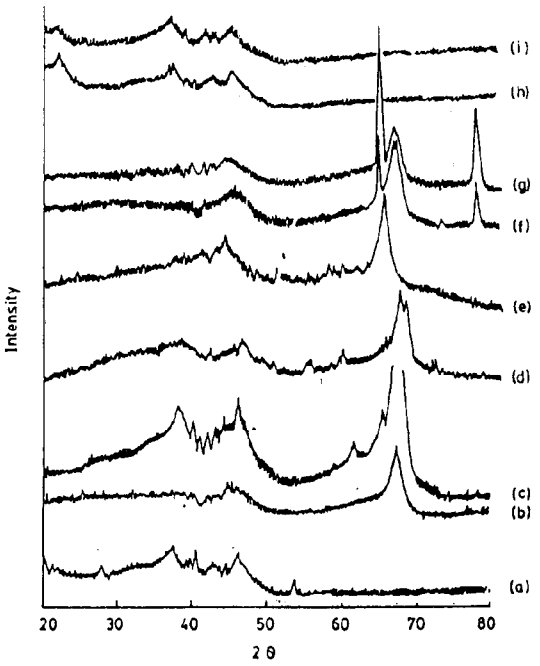

Fig. 1: XRD pattern for:
(a), Alumina; (b), $Cr_{0.0086}$ - Al_2O_3 ; (c), $Cr_{0.0417}$ - Al_2O_3 ;
(d), $Mn_{0.009}$ - Al_2O_3; (e), $Mn_{0.0439}$ - Al_2O_3 ; (f), $Fe_{0.009}$ - Al_2O_3
(g), $Fe_{0.0435}$ - Al_2O_3; (h), $Co_{0.0089}$ - Al_2O_3 ; (i), $Co_{0.0436}$ - Al_2O_3 3

doped alumina samples. It is noted that parent alumina as well as metal doped alumina samples show crystalline behavior by giving well defined spectra. Fig. (1) also shows the 2θ range in which spectra are obtained for parent and metal doped alumina samples. On doping the spectra range varies from metal to metal. However, range for the same metal of different concentration to some extent remains the same. From the X-ray diffraction pattern, it is obvious that 2θ range for parent alumina varies from 20-46°. Whilst for Cr, Mn, Fe and Co doped alumina samples, the 2θ range varies from 41-73°, 39-67°, 40-78° and 22-45° respectively. This variation indicates that the spectra range of all the metal doped samples is different than that of the parent alumina. Therefore, it can be concluded that behavior of the system is changing with doping.

The interlayers spacing d, the glancing angle θ and the x-ray wavelength λ, are related through the well known Bragg's law given by the equation below

from which d of the parent and metal doped alumina samples is calculated.

$$n\lambda = 2d \sin\theta \quad (1)$$

Where n is the order of the diffraction, λ is the wavelength of diffracted x-rays and diffracting planes. The d values of alumina samples for different hkl (Miller Indices), and the values of lattice constant and density for individual reflection and other calculated parameters are presented in Table (1). Results summarized in the said table do indicate modification of the surface properties of γ-alumina with metal loading.

Density of the parent and doped alumina samples is calculated by the equation.

$$\rho = \frac{nM}{a^3 N_o} \quad (2)$$

Where N_o is Avogadro's number, M the formula weight of the species associated with each lattice point, ρ th density and n the net number of lattice points per unit cell in the macroscopic crystal. If a single atom or molecule is associated with each lattice point, n = 1 for primitive cubic, n = 2 for body centered cubic and n = 4 for face centered cubic and

Table 1 X-ray diffraction data for metal doped alumina

Sample	2θ°	Interlayer spacing d(°A)	Miller indeces	Unit cell constt. a(nm)	Unit cell volume $a^3(nm^3)$	Density $\rho(g/cm^3)$	I/I_o
Alumina	20.40	0.4354	111	0.7541	0.4289	0.3947	0.8989
	27.98	0.3189	220	0.9020	0.7338	0.2307	0.7528
	37.85	0.2377	311	0.7884	0.4899	0.3455	0.9888
	39.60	0.2276	400	0.9104	0.7546	0.2243	0.8539
	40.05	0.2252	222	0.7801	0.4748	0.3565	0.8270
	40.70	0.2217	400	0.8868	0.6974	0.2427	1.0000
	43.10	0.2099	400	0.8396	0.5918	0.2860	0.8315
	46.26	0.1963	400	0.7852	0.4841	0.3497	0.9663
$Cr_{0.0086}$-Al_2O_3	41.65	0.2169	222	0.7514	0.4242	0.3993	0.7143
	58.60	0.1575	511	0.8184	0.5481	0.3102	0.5604
	60.40	0.1533	511	0.7966	0.5054	0.3364	0.5440
	66.28	0.1410	440	0.7976	0.5074	0.3351	1.0000
	71.00	0.1328	440	0.7512	0.5239	0.3245	0.4286
	72.75	0.1300	533	0.8525	0.6195	0.2745	0.4231
$Cr_{0.0417}$-Al_2O_3	41.50	0.2176	400	0.8704	0.6594	0.2622	0.5867
	46.02	0.1972	400	0.7888	0.4908	0.3523	0.6733
	59.40	0.1556	511	0.8085	0.5285	0.3272	0.5267
	67.20	0.1393	440	0.7879	0.4893	0.3533	1.0000
	67.76	0.1383	440	0.7823	0.4788	0.3611	0.9400
	73.18	0.1293	533	0.8478	0.6095	0.2836	0,4267
$Mn_{0.009}$-Al_2O_3	39.62	0.2275	222	0.7881	0.4895	0.3475	0.6700
	40.65	0.2220	222	0.7690	0.4548	0.3740	0.5800
	41.50	0.2176	400	0.8704	0.6594	0.2579	0.6100
	42.52	0.2126	400	0.8504	0.6149	0.2766	0.6400
	45.58	0.1990	400	0.7960	0.5044	0.3373	0.8000
	61.25	0.1513	511	0.7862	0.4859	0.3501	0.5250
	67.18	0.1394	440	0.7885	0.4904	0.3469	1.0000
$Mn_{0.0439}$-Al_2O_3	39.48	0.2283	222	0.7908	0.4946	0.3505	0.4660
	40.02	0.2253	222	0.7804	0.4754	0.3646	0.4757
	41.72	0.2165	400	0.8660	0.6495	0.2669	0.4466
	45.42	0.1997	400	0.7988	0.5097	0.3401	05476
	67.18	0.1394	400	0.7885	0.4904	0.3535	1.0000
$Fe_{0.009}$-Al_2O_3	40.15	0.2246	222	0.7780	0.4709	0.3613	0.3969
	41.95	0.2154	400	0.8616	0.6396	0.2659	0.3937
	45.65	0.1988	400	0.7952	0.5028	0.3383	0.4693
	48.70	0.1870	400	0.7840	0.4185	0.4065	0.2835
	65.04	0.1434	440	0.8112	0.5338	0.3187	1.0000
	67.18	0.1394	440	0.7885	0.4904	0.3469	0.9134
	78.12	0.1224	533	0.8026	0.5171	0.3290	0.5433

Table 1 Continued .....

Sample	2θ°	Interlayer spacing d(nm)	Miller indeces	Unit cell constt. a(nm)	Unit cell volume $a^3(nm^3)$	Density $\rho(g/cm^3)$	I/I_o
$Fe_{0.0435}$ -Al_2O_3	40.00	0.2254	222	0.7808	0.4760	0.3643	0.2180
	41.68	0.2167	222	0.7506	0.4230	0.4099	0.2150
	43.00	0.2104	400	0.8416	0.5961	0.2908	0.2120
	64.80	0.1439	440	0.8140	05394	0.3215	1.0000
	67.06	0.1396	440	0.7896	0.4925	0.3512	0.4000
	78.02	0.1225	533	0.8033	0.5183	0.3345	0.5150
$Co_{0.0089}$ -Al_2O_3	22.06	0.4030	111	0.6980	0.3401	0.5006	1.0000
	37.13	0.2422	311	0.8033	0.5183	0.3284	0.8830
	39.15	0.2301	222	0.7971	0.5064	0.3361	0.7774
	40.00	0.2254	222	0.7808	0.5460	0.3117	0.7358
	42.70	0.2118	400	0.8472	0.6080	0.2799	0.8058
	45.20	0.2006	400	0.8020	0.5166	0.3295	0.8264
$Co_{0.0436}$ -Al_2O_3	22.10	0.4023	111	0.6968	0.3383	0.5134	1.0000
	37.25	0.2414	311	0.8006	0.5132	0.3383	0.9756
	39.00	0.2309	311	0.7658	0.4491	0.3866	0.8537
	41.30	0.2186	222	0.7573	0.4342	0.3998	0.8293
	42.80	0.2113	400	0.8452	0.6038	0.2875	0.8415
	45.02	0.2014	400	0.8056	0.5228	0.3321	0.9024

a^3 is unit cell volume calculated by cube square of unit cell constant. The value of a, the lattice constant, the length of the edge of the unit cell is calculated by an equation [25-28].

$$a = d\,(h^2 + k^2 + l^2)^{1/2} \qquad (3)$$

Where d is the interplanar spacing of the diffracting planes (A°) and hkl are the miller indices of the plane.

Table (1) also reports that peak of maximum intensity for pure Al_2O_3 is observed at 40.70 for which $I/I_o = 1$. Whilst for Cr, Mn, Fe and Co doped alumina samples, the peak of maximum intensities are observed at 66-67°, 45°, 65° and 22.06° respectively. Which indicates that impregnation of alumina with different metal concentration create additional phase changes at the level of detection of XRD. This shows that metal residues may be present on the surface of alumina in the dispersed form. This idea of presence of metal resides in dispersed form is further supported by the nitrogen adsorption study as discussed in our previous paper [10]. Nitrogen adsorption study reveals that metal residues exist at alumina pore entrance leading to an appreciable pore blockage.

The unit cell dimension for parent and metal doped alumina samples are also calculated by using computer program. The program requires the input data in the form of trial values of lattice parameters, observed d or 2θ values with corresponding hkl indices. The output consists of observed and calculated 2θ and d and hkl indices, usually after two or three refinement cycles, refined cell parameters for a particular crystal lattice are obtained. The values of unit cell constant, unit cell volume, densities and the mean crystallite size determined by this method are given in the Table (2). Thus X-ray diffraction line broadening method was employed to determine the mean crystallite size of the doped alumina samples where it was possible. For the determination of crystallite size as determined by the broadening of the diffraction rings, many authors [29-35] have advanced theories and equations. These equations differ mainly in the basic assumption as to crystallite shape, separation and mode of packing. However, assuming spherical crystallite with random packing, the required relation for the estimation of average crystallite size composing a powder is given by the Scherrer equation

$$B_c = \frac{K_1 \lambda}{d\,\mathrm{Cos}\theta} \qquad (4)$$

Where B_c is the line broadening, K_1 a constant (0.893), λ the wavelength of x-radiation employed (A°),d the crystallite size (A°) and θ the Bragg's

Table-2: X-Ray Diffraction data for metal doped alumina

Sample	Unit Cell constant a(nm)	Unit cell volume $a^3(nm^3)$	Density (gm/cm^3)	Mean crytallite size (nm)
Alumina	0.8298	0.5729	0.2964	0.8166
$Cr_{0.0086}$-Al_2O_3	0.8063	0.5243	0.3244	-
$Cr_{0.0417}$ -Al_2O_3	0.7973	0.5068	0.3413	-
$Mn_{0.009}$-Al_2O_3	0.8047	0.5210	0.3266	-
$Mn_{0.0419}$-Al_2O_3	0.8017	0.5153	0.3366	-
$Fe_{0.009}$ -Al_2O_3	0.8091	0.5296	0.3214	0.8492
$Fe_{0.0435}$ -Al_2O_3	0.8005	0.5130	0.3381	0.9030
$Co_{0.0089}$-Al_2O_3	0.8074	0.5264	0.3235	-
$Co_{0.0436}$-Al_2O_3	0.7979	0.5081	0.3418	-

angle at which measured reflection is occurring. It is observed that doping of alumina affects its interlayers spacing and the structure of alumina is distorted. This behavior is true for all metals.

The technique of mercury intrusion under pressure provides meaningful information about the pore size distribution in the macropore-range of porous solids. Since its discovery, the technique has been developed and improved to the extent that it is theoretically possible to determine the quantity of pore spaces in porous materials, the density of both solids objects and powders, the pore specific surface area, a measure of particle size distribution in case of porous powders and information about the shape and structure of pores [14, 18, 21, 36-39].

Washburn [14] pointed out the fact that surface tension opposes the entrance into a small pore of any liquid having an angle of contact greater than 90°; and this opposition may be overcome by the application of external pressure. Washburn also proposed that for a constant surface tension and contact angle, the diameter of a pore enterable by mercury is a direct function of the applied pressure. As the pressure is increased, the mercury penetrates into smaller pores in response to their size and to the applied pressure [1,13,40]. Henderson, Ridgway and Ross [41] have used this principle in a limited way, and Loisy [42] has proposed the use of the same principle in a study of pore size distribution. Mercury [1] exhibits a greater contact angle with a large number of materials than any other conveniently useable liquid. Thus, it is the most suitable liquid for the evolution of porous materials. In the present work, it is applied to determine pore size distribution in the parent and metal (particularly Cr) doped alumina samples.

Figs. (2-4) are the plots (pore size distribution curves) of typical intrusion (v_{int}) and extrusion (v_{ext}) volume as a function of applied pressure for parent and Cr doped alumina ($Cr_{0.0086}$-Al_2O_3 & $Cr_{0.0417}$-Al_2O_3) samples. The measured quantity of mercury forced to intrude into the pores of pure and metal doped alumina samples against applied pressure and then to extrude exhibit hysteresis, the lower branch of which represents measurements obtained by progressive addition of mercury to the system and the upper branch represents measurements obtained by progressive withdrawal from the alumina samples. Hysteresis so obtained indicates that mercury extrusion does not follow the path of mercury intrusion. The reason for this is that extrusion of mercury from alumina samples does not occur as easily as intrusion. This is because intrusion pressure is always greater than extrusion pressure. Hence hysteresis results [43].

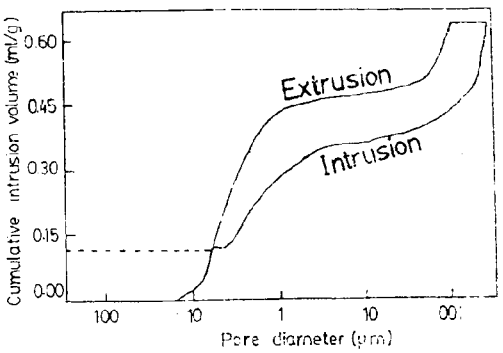

Fig. 2. Mercury intrusion and extrusion curves for parent alumina

The first plot Fig.(2) of typical intrusion (v_{int}) and extrusion (v_{ext}) volume for parent alumina shows that there is a steep initial region in the intrusion curve (pressuring plot) which at higher pressure abruptly goes down for a short distance. However, as the applied pressure increases further, there is again relatively sharp increase in the intrusion of mercury into the pores of alumina samples. The initial steep slope of the intrusion plot may be due to penetration of mercury into the largest pores as well as into the interparticulate spaces and interstices between particles [10,44,45]. Once the mercury has got entry into the largest pores, interparticulate spaces and interstices, the slope of the plot flattens. As the pressure is further increased, mercury is forced progressively to intrude the extremely fine and smaller pores having restricted openings. Above particular pressure no appreciable intrusion takes place. The extrusion curve shows that mercury

extrusion does not follow the same path and after a small decrease in intruded volume at high pressure, no further mercury extrusion occurs. Thus, it is observed that after penetration and retraction approximately 16% of the mercury is retained by the pores of parent alumina. The flat area of the hysteresis of the extrusion curve represents the filling of all the pores. Ritter and Drake [15,40] found in their original work that the curves of volume against pressure for the penetration and withdrawal did not coincide. Numerous investigations since then have confirmed that hysteresis is a general feature of mercury porosimetry, for which the intrusion pressure is greater than extrusion and hence there will be hysteresis [16].

It is also obvious from irreversibility of the hysteresis that pores of the alumina samples are not cylindrical in nature. If the pores are assumed to be right cylindrical with constant cross section and with the same advancing and receding contact angle, then the point of penetration and retraction of mercury will fall on the same line and there will be no hysteresis.

The second plot Fig (3) for $Cr_{0.0086}$-Al_2O_3 shows the same behavior as shown by parent alumina, except that there is a steep initial portion in the intrusion plot which gradually goes down at higher pressure and also that 49% of the mercury is retained in the pores of chromium doped sample. However, as the applied pressure increases further, sharp increase in the intrusion of mercury is observed and ultimately slope of the intrusion plot flattens

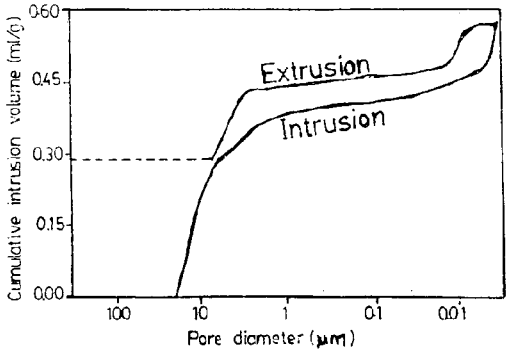

Fig. 3. Mercury intrusion and extrusion curves for $Cr_{0.0086}$ - Al_2O_3

The third plot Fig. (4) for $Cr_{0.0417}$-Al_2O_3 behaves like $Cr_{0.0086}$-Al_2O_3 and also that 59% of the

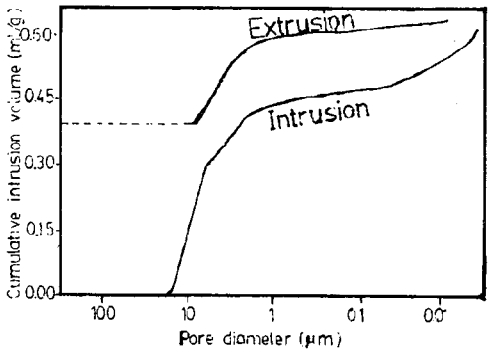

Fig. 4. Mercury intrusion and extrusion curves for $Cr_{0.0086}$ - Al_2O_3

mercury is retained in the pores of chromium doped samples. Emmett [46] reported that the mercury is not completely removed from the pores because the pore system deviate from the simple picture of cylindrical pores. According to Zhdanov, [46] the fraction of mercury retained in the pores may vary depending upon the nature of pores of adsorbents. The most extensive study of hysteresis in high pressure was made by Kamakin [47] who used an alumina-silica sample. Kamakin is of the view that the irreversibility of hysteresis is due to the fact that (for instance a very long equilibrium time) mercury cannot be reversibly retracted from pores with minimum opening r~75A°. It is also observed that the sample showing the lower mercury hysteresis are those that exhibit little or no water hysteresis [48].

The best explanation of hysteresis in mercury porosimetry is based on the "ink-bottle" model. The irreversibility is due to the existence of these "ink-bottle" pores (composed of cylindrical pore closed at one end and with a narrow neck at the other end) in the parent and metal doped alumina samples. These" ink bottle" pores are wider in the interior than at the exit, so that mercury cannot intrude until the pressure has risen to the value corresponding to the radius of the entrance capillary. Once the pressure is progressively increased and realized, wider and wider pores are filled until at the saturation pressure the entire system is full of mercury, thus giving an erroneously high apparent pore volume of capillaries of that size. Such a situation leads to a hysteresis effect i.e. on reducing the applied pressure, mercury can not leave the entrance capillary due to the presence of ink bottle pores until the pressure has fallen to appropriate value.

The pore size distribution (distribution of pore volume with respect to pore size) for pure and Cr doped alumina samples as determined from mercury penetration is compared and is given in histogram, Fig. (5). for parent alumina, for $Cr_{0.0086}$-Al_2O_3 and $Cr_{0.0417}$-Al_2O_3. This is a plot of differential volume dv/dD (ml/g-μm) vs pore diameter r (μm) i.e. applied pressure. Mercury is transferred into the pores of alumina samples as a function of the effective radii "r". The analysis of this histogram gives an idea about the effect of metal doping on the mesopore and macropore of alumina. It can be observed that the mesopore volume of alumina decreases with the increasing amount of doped metal in the alumina. It indicates that pore size decreases as metal concentration increases. This may be due to the dispersion of metal residues on the surface of alumina. This effect is very small at low metal concentration, but high as the metal concentration increases

The data in table (3) of the current paper shows that total pore area decreases with increase in the amount of doped metal. It can be said that these metals do not contribute any extra surface to the alumina. This decrease in surface area with the increasing amount of the metal may be due to dispersion of metal residues on the surface of alumina and different degree of dispersion reflects a property of the doped material itself [49,50].The idea of presence of metal residues on the surface of alumina in dispersed form is consistent with pore size distribution curve, Fig.(5).

Table 3:Results of preparation and analysis of metal doped alumina

Sample tried to prepare	Ratio of Doped to Charged metal	Composition of doped alumina	Pore area ($m^2 g^{-1}$) of doped alumina
Al_2O_3	____	____	200.12
$Cr_{0.01}$-Al_2O_3	0.865	$Cr_{0.0086}$-Al_2O_3	129.51
$Cr_{0.05}$-Al_2O_3	0.833	$Cr_{0.0417}$-Al_2O_3	92.27
$Mn_{0.01}$-Al_2O_3	0.900	$Mn_{0.009}$-Al_2O_3	174.84
$Mn_{0.05}$-Al_2O_3	0.877	$Mn_{0.0439}$-Al_2O_3	136.11
$Fe_{0.01}$-Al_2O_3	0.900	$Fe_{0.009}$-Al_2O_3	158.59
$Fe_{0.05}$-Al_2O_3	0.870	$Fe_{0.0435}$-Al_2O_3	109.64
$Co_{0.01}$-Al_2O_3	0.893	$Co_{0.0089}$-Al_2O_3	146.86
$Co_{0.05}$-Al_2O_3	0.872	$Co_{0.0436}$-Al_2O_3	117.69

Experimental

Material

Alumina was supplied by Fluka (item # 06290) , Chromium Chloride (Item # 2487) and Iron Chloride (Item # 3943) were supplied by Merck whilst Manganese Chloride (Item # 63543) and Cobalt Chloride (Item # 60820) were supplied by Fluka with purities better than 99%.

Preparation of adsorbents

For the preparation of metal impregnated alumina samples [51-53], a pre-determined amount of metal chloride was magnetically stirred in 200 ml of doubly distilled water and 20 g of alumina was added to the mixture. The mixture was stirred for about 8 hours at 373K till a slurry was formed. The excess solution was then driven off through vacuum desiccator connected with a suction pump. The

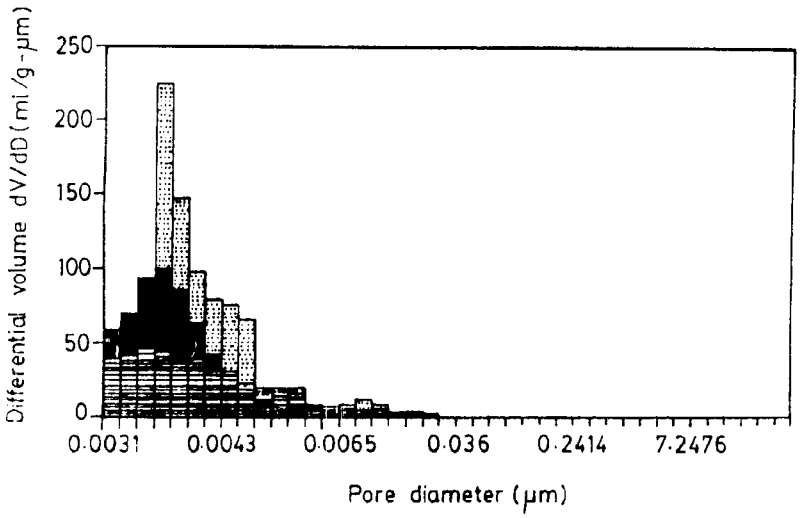

Fig. 5. Pore size distribution for: (▨), Alumina; (■), $Cr_{0.0086}$ - Al_2O_3 ; (▤), $Cr_{0.0417}$ - Al_2O_3

samples were then dried at 373K for 3 hours. A blank alumina sample was also prepared by giving the same treatment except that distilled water was used in place of metal chloride solution. Two samples of different concentrations for every metal were prepared. A summary of the samples whose preparation was attempted and the composition as well as analysis of the doped materials obtained is given in Table (3).

The metal impregnated alumina were designated by the following formulae M_x-Al_2O_3, where M stands for Cr, Mn, Fe and Co and x represents the number of moles per 100g of alumina.

Determination of the amount of metal in the alumina supported metal adsorbents

For the measurement of metal concentration, 1g of the sample was thoroughly stirred with nitric acid solution for 4 hours at room temperature. The mixture was then filtered and the residue treated once more with nitric acid solution. The procedure was repeated four times. After extraction, the solution was made upto the required volume with deionized water. The total amount of the metal in the solution was then determined by atomic absorption spectrophotometery (Shimadzu AA-670 model instrument).

X-ray diffraction studies

In the present work, diffraction patterns of all the metal loaded alumina samples and of the parent alumina were obtained with a Phillips PW 1050 diffractometer. The detector was xenon proportional counter linked to PW 4620 ratemeter and channel analyzer. The radiation was graphite monochromatized Cuk_α (1.5418 A°), generated in a Philips 1130/80, operated at 40 kV and 20 mA. The diffractometer was operated at 1.0° diverging and 0.1° receiving slits at a scan rate of 2 deg/min. The continuous traces of x-ray reflection were obtained from flat surface of the alumina samples pellets, since this technique was found to give more reproducible results than powder samples. The scattered beam was detected with the help of a detector positioned at an angle of 2θ with respect to the primary beam direction. The position of maximum intensity peak, the 2θ values and the d values were also calculated and presented.

Mercury porosimetric measurement

This experiment was conducted using a Micrometrics Mercury Penetration Porosimeter, Model 9220 Autopore II. All the metal loaded alumina samples were dehydrated and dried in a vacuum oven at 333K over night. A weight of 0.1-0.4g of dried sample was used for porosimetric measurement. Mercury having surface tension 485.00dynes/cm and contact angle 130° was used.

Conclusions

A detailed examination of x-ray diffraction indicates that properties of γ-alumina are changed with metal doping. X-ray diffraction analysis on the impregnated alumina samples also reveals the existence of crystalline material. From the results of mercury penetration, it has been noted that mercury intrusion and extrusion curves are irreversible, giving the evidence of "ink bottles" pores in the alumina samples. From the data, it has also been observed that pore size of the alumina samples decreases with increasing metal concentration.

Acknowledgements

One of us (A.K.K.) gratefully acknowledges his indebtedness to the University Grants Commission Islamabad, for financial support which supported the work presented in the paper. He also wishes to express his thanks to Dr. Khalil Qureshi (Dir.), New Laboratories, Pakistan Atomic Energy Commission for providing laboratory facilities.

References

1. A.A. Liabastre and C. Orr, *J. Colloid Interface Sci.*, **64**, 01 (1978).
2. M. Saleem, M. Afzal and F. Mahmood, *Adsorption Sci. and Technol.*, **9**, 17 (1992).
3. B. Boddenberg and B. Beerwerth, *J. Phys. Chem.*, **93**, 1435 (1989).
4. M. Afzal, M. Khan and H. Ahmad, *Colloid Polym. Sci.*, **269**, 483 (1991.
5. M. Saleem, M. Afzal, T.M. Naeem and F. Mahmood, *Adsorption Sci. Technol.*, **11**, 95 (1994).
6. M. Afzal and M. Khan, *J. Chem. Soc. Pak.*, **9**, 337 (1987).
7. S. Brunauer, R.Sh. Mikhial, and E.E. Bodor, *J. Colloid Interface Sci.*, **24**, 451 (1967).
8. M. Afzal, F. Mahmood and M. Saleem, *Carbon*, **31**, 01(1993).
9. A.K. Khattak, M. Afzal, M. Saleem, G. Yasmeen and J. Afzal, *Adsorption Sci. Technol.*, **17**, 181(1999).
10. A.K. Khattak, M. Afzal, M. Saleem, G. Yasmeen and R. Ahmad, *Colloids Surf.*, **162**, 99 (2000).

11. A.K. Khattak, K. Mahmood, M. Afzal, M. Saleem, and G. Yasmeen, *Separation Sci. Technol.*, **37 (6)**, 1 (2002).
12. J.E. Huheey, E.A. Keiterand and R.L. Keiter, Inorganic Chemistry: Principles of structure and reactivity, 4th Ed., Harper Collins College Publishers (1993).
13. A.J. Juhola and E. O. Wing, *J. Am. Chem. Soc.*, **71**, 2078 (1949)
14. E.W. Washburn, *Proc. Natl. Acad. Sci.* USA, **7**, 115 (1921); Washburn and E.N. Bunting, *J. Am. Ceramic Soc.*, **5**, 48 (1922).
15. H.L. Ritter and L.C. Drake, *Ind. Eng. Chem. Anal. Ed.*, **17**, 782, 787 (1945).
16. Emmett, Holmes and Mace, OSRD Formal Report (1943).
17. C.N. Cochran and L.A. Cosgrove, J. *Phys. Chem.*, **61**, 1417 (1957).
18. C. Orr Jr. and J..M. Dalla Valle,."Fine Particle Measuremen" Macmillan New York (1959).
19. A.H. Ellision, R.B. Klemn, A.M. Schwartz, L.S. Grubb and D.A. Petrash, *J. Chem. Eng. Data*, **12**, 607 (1967).
20. L.G. Joyner, E.P. Barrett and R. Skold, *J. Amer. Chem. Soc.*, **73**, 3155 (1951).
21. H.M. Rootare, *Aminco Laboratory News*, **24**, (3), Fall (1968).
22. M. H. Jellinek and I. Fankuchen, *Ind. Eng. Chem.*, **37**, 158 (1945.
23. R. Brill, *Z. Krist*, **83**, 323 (1932).
24. G. Hagg, and G. Soderholm, *Z. Physik. Chem.*, **B29**, 88 (1935).
25. J..M. White, Physical Chem. Lab. Experiments, University of Texas, Austin, (1975).
26. F. Daniels and Mcgrawhill, Experimental Physical Chemistry, 7th Ed. Londonm, Panama, (1970).
27. A.R. Verma and O.N. Srivastava, Crystallography for solid state Physics, Wiley Eastern Limited, New Delhi, 1987.
28. M.K.B. Day and V.J. Hill, *J. Phys. Chem.*, **57**, 946 (1953).
29. G.C. Bond, Heterogeneous Catalysis, Principles and Applications, 2nd. Ed. Oxford Chemistry Series (1987).
30. G. H. Cameronand and A.L. Patterson, Am. Soc.,Testing Materials, Symposium on Radiography and X-Ray Diffraction Methods, (1936).
31. K.H. Meyer, Natural and Synthetic High Polymers, Interscience Pub., New York (1942).
32. C. C. Murdock, *Phys. Rev.*, **35**, 8 (1930).
33. J. Biscoe and B.E. Warren, *J. Applied Phys.*, **13**, 364 (1942).
34. Scherrer in Zsigmondy's "Kolloidchemie", (1922).
35. H. Klug and L. Alexander, X-ray Diffraction Procedures, John Wiley, New York. (1954).
36. H. Marsh and B. Rand, *J. Colloid Interface Sci.*, **33**, 101 (1970).
37. M. Svata, *Powder Technol.*, **5**, 345 (1971).
38. C. Orr and Jr., *Powder Technol.*, **3**, 117 (1969).
39. A. Kiselev, "The structure and Properties of Porous Materials", (D.H. Everett, F.S. Stone, Eds.), Butterworth, London, (1958).
40 L.C. Drake, *Ind. Eng. Chem.*, **41**, 780 (1949).
41. L.M. Henderson, C..M. Ridgway and W.B. Ross, *Refiner*, **19**, 185 (1940).
42. R. Loisy, *Bull. Soc. Chem.*, **8**, 589 (1941).
43. S.J. Gregg and K.S.W. Sing, Adsorption, Surface Area and Porosity, 2nd. Ed. Academic Press Inc., London (1982).
44. M. Afzal, F. Mahmood and M. Saleem, *J. Chem. Soc. Pak.*, **15**, 100 (1993).
45. S.J. Gregg, K.S.W. Sing and H.F. Stoeckli, *Soc. Chem. Ind.*, London (1979).
46. Emmett, *Chem. Rev.*, **43**, 69 (1948); S.P. Zhdanov "Methods of study of the structure of highly dispersed and porous materials - Paper of the 2nd conference", Editor, M. M. Dubinin, Izd. Aka. Nauk., Mascow, (1958).
47. N.N Kamakin "Methoden der Strukturuntersuchung an Hoechdispersen und Porosen Stoffen" (Translated from a Russian Edition by Witzmann, H) Alkademie-Verlag. Berling, (1961).
48. R.M. Barrer, N. Mckenzie and J.S.S. Reay, *J. Colloid. Sci.*, **11**, 497 (1956).
49. M. Afzal and F. Mahmood, *Collect. Czech. Chem. Commun.*, **58**, 474 (1993).
50. M. Saleem, M. Afzal, H. Ahmad and M. Sulaiman, *Phys. Chem.*, **10**, 11(1991).
51. M. Afzal, F. Mahmood and M. Saleem, *Ber. Bunsenges Phys.Chem.*, **96**, 693 (1992).
52. M. Afzal, F. Mahmood and M. Saleem, *Colloid Polym. Sci.*, **270**, 917 (1992).
53. M. Afzal, F. Mahmood and H. Ahmad, *Colloids and Surf.*, **66**, 287 (1992).